

Precision Measurement of a Particle Mass at the Linear Collider

C. Milténe¹, A. Freitas², M. Schmitt³, A. Sopczak⁴ *

1-Fermi National Laboratory- Batavia-IL-60510 -USA.

2-Institut für Theoretische Physik, Universität Zürich,
Winterthurerstrasse 190, CH-8057, Zürich, Switzerland.

3- Northwestern University, Evanston, USA.

4- Lancaster University, Lancaster LA1 4YB, United Kingdom.

Precision measurement of the stop mass at the ILC is done in a method based on cross-sections measurements at two different center-of-mass energies. This allows to minimize both the statistical and systematic errors. We obtain a much better stop mass precision than in previous studies. In the framework of the MSSM, a light stop is studied in its decay into a charm jet and a neutralino, the Lightest Supersymmetric Particle, as a candidate of dark matter. This takes place in the co-annihilation region, namely, for a small stop-neutralino mass difference.

1 Introduction

In this study we are aiming at the minimisation of the systematic uncertainties as well as the statistical error [1]. This is achieved by using a method which allows to increase the precision in two ways. We will deal with a ratio of cross-sections at two energy points. This will take care of the systematic uncertainties by cancelations and then, we choose one of the energies to be at the threshold where the sensitivity to mass is maximale. We will show that even though we are dealing with more realistic data than in [2], we improve substantially the precision in the mass measurement. As in [2], we are considering the MSSM with R Parity conservation and a scenario in which a light stop co-annihilates with the Lightest Supersymmetric Particle (LSP), the neutralino, to produce the right amount of dark matter relic density, namely, within the experimental precision of WMAP and the Sloan digital sky survey [3]. Together with a light Higgs, a light right-handed stop also supports electroweak baryogenesis. Our data now include hadronization and fragmentation of the stop before its decay as well as fragmentation of the charm of the decay. This provides a rather big smearing of the particles produced and increases the number of jets. We will use two different approaches. First we will optimize a set of sequential cuts as in [2], then we will be using a multi-variable optimization, of the neural-network type IDA. We do take also advantage of the polarization since we deal with an almost right-handed stop as required for E.W. baryogenesis. This allow us to enhance the signal while getting rid of a big part of the main background.

2 Mass Precision Measurement: the Method

- The production cross-section of stop pairs $e^+e^- \rightarrow \tilde{t}_1 \tilde{t}_1^*$ is represented to next to leading order (NLO), as a function of the energy for two hypothetical values of the stop mass, 122.5 GeV and 123.5 GeV, shown in Figure 1.

*presented by A. Sopczak

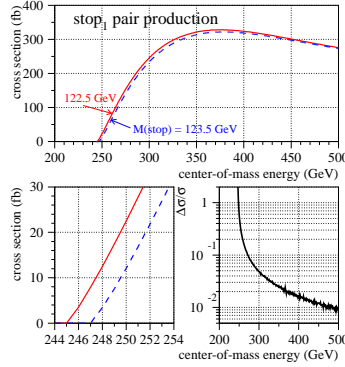


Figure 1: Precision in Pair Production Cross-Section

- In the lower left figure the scale has been blown up and one can see that the sensitivity to small mass difference is high at or close to threshold while in the lower right figure one sees that it is not the case at peak value.
- We will define a parameter Y , as a ratio of production cross-sections at two energy points. This will reduce the systematic uncertainties in Y from the efficiencies as well as from the beam luminosity measurements between the two energy points.
- One of the energy points is chosen at or close to the production energy threshold. This provides an increased sensitivity of Y to mass changes.

$$Y(M_X, \sqrt{s_{th}}) \equiv \frac{N_{th} - B_{th}}{N_{pk} - B_{pk}} = \frac{\sigma(\sqrt{s_{th}})\epsilon_{th}L_{th}}{\sigma(\sqrt{s_{pk}})\epsilon_{pk}L_{pk}} \quad (1)$$

σ is the cross-section in [fb], N the number of detected data, B is the number of estimated background events, s is the square of the center of mass energy, ϵ the total efficiency and acceptance and L is the integrated luminosity. The suffix (th) is used for the point at energy threshold and (pk) for the energy peak. M_x is the mass to be determined with high precision.

In the method, we determine the stop mass by comparing Y with the theoretical calculation of the cross-sections to next to the leading order (NLO) for both QCD and QED. It has been done for +80% polarizations for the e^- beam and -60% polarization for the e^+ .

3 The Channel Studied $e^+e^- \rightarrow \tilde{t}_1 \tilde{t}_1^* \rightarrow cX^0 \bar{c}\bar{X}^0$

A scan in the super-symmetry parameter space [5] has shown that a stop mass of 122.5 GeV and a neutralino mass of 107.2 GeV are consistent with baryogenesis and dark matter. The process and the background channels are listed below with their cross-sections with and without polarisation.

3.1 Simulations Characteristics

The signal and background channels were generated with Pythia(6.129), the simulator Simdet(4.03) and for the beamstrahlung Circe(1.0)[6]. They were generated in proportion

Process	Cross-section [pb] at $\sqrt{s} = 260$ GeV			Cross-section [pb] at $\sqrt{s} = 500$ GeV		
$P(e^-)/P(e^+)$	0/0	-80%/+60%	+80%/-60%	0/0	-80%/+60%	+80%/-60%
$t_1 t_1^*$	0.032	0.017	0.077	0.118	0.072	0.276
$W^+ W^-$	16.9	48.6	1.77	8.6	24.5	0.77
ZZ	1.12	2.28	0.99	0.49	1.02	0.44
$We\nu$	1.73	3.04	0.50	6.14	10.6	1.82
eeZ	5.1	6.0	4.3	7.5	8.5	6.2
$q\bar{q}, q \neq t$	49.5	92.7	53.1	13.1	25.4	14.9
$t\bar{t}$	0.0	0.0	0.0	0.55	1.13	0.50
2-photon $p_t > 5$ GeV	786			936		

Table 1: The Cross-sections at $\sqrt{s} = 260$ GeV and $\sqrt{s} = 500$ GeV for the signal and Standard Model background are given for different polarization combinations. The signal is given for a stop mixing angle of 0.01 and for a stop of $m_{\tilde{t}} = 122.5$ GeV, consistent with E.W. baryogenesis. The e^- negative polarization values refer to left-handed polarization and positive values to right-handed polarization.

with their cross-sections.

- Hadronization of the \tilde{t}_1 quark and the fragmentation of the charm quark come from the Lund string fragmentation model. We use Peterson fragmentation [7].
- The stop fragmentation is simulated using T. Sjostrand's code [6]. The stop quark is set stable until after fragmentation, then it is allowed to decay as described in detail by A.C.Kraan[7]. The stop fragmentation parameter is set relative to the bottom fragmentation parameter $\epsilon_{\tilde{t}} = \epsilon_b m_b^2 / m_{\tilde{t}}^2$ and $\epsilon_b = -0.0050 \pm 0.0015$. The charm fragmentation is set from LEP to $\epsilon_c = -0.031 \pm 0.011$.
- The mean jet multiplicity increased for the data with fragmentation included.

4 The Analysis

The ntuple analysis code [8] which incorporates the Durham jet algorithm is used. The pre-selection and selection cuts are described in detail at both energies in [9].

4.1 The sequential cuts

Were made as similar as possible at the two energies to aim at the cancellation in Y of the systematics. The cuts and their detailed results are given in [9].

After performing the cuts and assuming for the beam e^- +80% polarisation and for e^+ -60% polarization we have at 260 GeV with 34% signal efficiency 1309 events for a beam luminosity of 50 fb^{-1} , with a background of 60 $We\nu$, 53 two-photons, 45 $q\bar{q}$ and a score of WW, ZZ, eeZ.

At 500 GeV, with the same beam polarizations and a luminosity of 500 fb^{-1} , the signal efficiency is 22% with 29270 events and a background including 5495 $We\nu$, 81 ZZ, 43 $q\bar{q}$, 31 two-photons, and a score of $t\bar{t}$.

4.2 Iterative Discriminant Analysis (IDA)

Combines the kinematic variables in parallel. The same variables and simulated events are used than in the cut-based analysis. A non-linear discriminant function followed by iterations enhances the separation signal-background. Both signal and background have

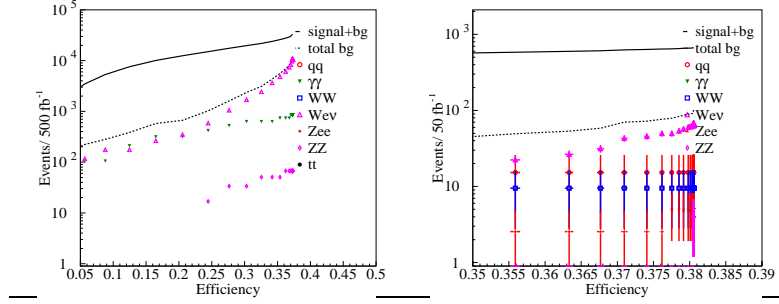


Figure 2: Detection Efficiency and Background Events at 500 GeV(left) and 260 GeV (right).

been divided in equally sized samples, one used for the training, the other as data. We will make two IDA iterations in our final analysis [9]. The results are shown after a first IDA iteration for which one keeps 99% of the signal efficiency followed by a second iteration. We assume the same luminosities and polarizations than for the sequential based analysis.

With a similar background the efficiency reached is 41.6% at 500 GeV (22% sequential cut) and 38.7% at 260 GeV (34% with sequential cuts).

Error source for Y	Cut-based analysis	Iterative Discriminant Analysis
Statistical	3.1%(0.19GeV)	2.7%(0.17GeV)
Detector effects(systematics)	1.0%	2.1%
Jet number (systematics)	1%	1%
Charm fragmentation (systematics)	0.5%	0.5%
Stop fragmentation(systematics)	2.7%	2.8%
Charm tagging algorithm (systematics)	< 0.5%	< 0.5%
Sum of experimental systematics	3%(0.18 GeV)	3.6%(0.22 GeV)
Sum of experimental errors	4.3%(0.26 GeV)	4.5%(0.28 GeV)
Theory for signal cross-section	5.5%	5.5%
Theory for background cross-section	2.0%	1.1%
Total error δY	7.3% (0.44 GeV)	7.2%(0.45 GeV)

Table 2: Combination of statistical and systematic errors for the determination of the stop mass from a threshold-continuum cross-section measurement. In parenthesis is given the overall error on the measured mass.

The next to next to leading order (NNLO) QCD corrections are expected to be of the same order than the NLO. This is based on the top quark results. Assuming a factor two improvement in the calculations by the time ILC is running (A 1% NNLO correction is assumed for the EW component). The relic dark matter density is shown below

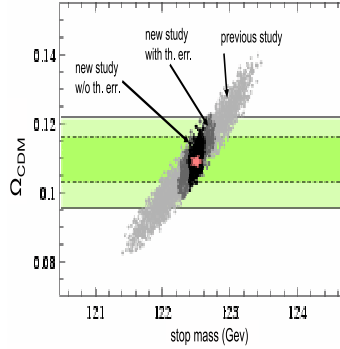


Figure 3: Dark matter Relic Density

5 Conclusions

We deal with more realistic data, including quarks hadronization and fragmentation but still manage to improve the stop mass precision by a factor three comparatively to [2]. The results for the mass precision are shown together with the dark Matter relic density in three cases for $\delta m_{\tilde{t}_1} = 0.44$ GeV, $\Omega_{CDM} h^2 = 0.109 + 0.0015 - 0.013$, it includes both experimental and theoretical errors. For $\delta m_{\tilde{t}_1} = 0.26$ GeV $\Omega_{CDM} h^2 = 0.109 + 0.0013 - 0.0010$, for experimental errors and sequential cuts and for $\delta m_{\tilde{t}_1} = 0.28$ GeV, $\Omega_{CDM} h^2 = 0.109 + 0.0013 - 0.0010$ as well for the IDA and experimental errors. The evolution in the precision of the dark matter relic density evaluation due to improvements in $\delta m_{\tilde{t}_1}$ is shown in the last figure.

References

- [1] Slides:
<http://ilcagenda.linearcollider.org/contributionDisplay.py?contribId=49&sessionId=69&confId=1296>
- [2] M. Carena, A. Finch, A. Freitas, C. Milstene, H. Nowak, A. Sopczak, Phys. Rev. **D72** 115008 (2005).
C. Milstène, M. Carena, A. Finch, A. Freitas, H. Nowak and A. Sopczak, in *Proc. of International Linear Collider Physics and Detector Workshop, Snowmass, Colorado, 14-27 Aug 2005*, eConf C0508141.
- [3] D. N. Spergel *et al.* [WMAP Collaboration], astro-ph/0603449. M. Tegmark *et al.* [SDSS Collaboration], Astrophys. J. **606**, 702 (2004).
- [4] G. Feldman, R. Cousins, Phys. Rev. **D57** 3873 (1998).
- [5] C. Balazs, M. Carena, C. Wagner) hep-ph/0403224v2-(2004).
- [6] T. Sjöstrand, P. Eden, C. Friberg, L. Lönnblad, G. Miu, S. Mrenna and E. Norrbin, Comput. Phys. Commun. **135**, 238 (2001); see also T. Sjöstrand, L. Lönnblad and S. Mrenna, hep-ph/0108264.(Pythia).
M. Pohl and H. J. Schreiber, hep-ex/0206009,(Simdet).
T. Ohl, Comput. Phys. Commun. **101**, 269 (1997),(Circe).
- [7] Peterson *et al.* Phys. Rev. **D27** 105 (1983),(Petersen). A. C. Kraan, Eur. Phys. J. C **37**, 91 (2004).
- [8] T. Kuhl, *N-Tuple working on Simdet DST structure*,
<http://www.desy.de/~kuhl/ntuple/ntuple.html>.
- [9] A. Freitas, C. Milstene, M. Schmitt, A. Sopczak. Publication with a complete description of the method and the analysis(in preparation).